



Collapse risk of tall steel moment-resisting frames in deep sedimentary basins during large magnitude subduction earthquakes

Carlos Molina Hutt¹, Shervin Zahedimazandarani², Nasser Marafi³, Jeffrey Berman⁴ & Marc Eberhard⁴

¹ Assistant Professor, Department of Civil Engineering, The University of British Columbia - Vancouver, BC.

² MSc Student, Department of Civil Engineering, The University of British Columbia - Vancouver, BC.

³ Post-Doctoral Researcher, Department of Civil & Environmental Engineering, The University of Washington - Seattle, WA.

⁴ Professor, Department of Civil & Environmental Engineering, The University of Washington - Seattle, WA.

ABSTRACT

Buildings in Seattle, WA have the potential to experience large-magnitude earthquakes generated by the Cascadia Subduction Zone, which is located approximately 100 km from the city. Furthermore, the city lies above a deep sedimentary basin which can amplify the intensity of earthquake ground motions at long periods and the resulting damage in tall structures. Steel moment-resisting frames are of importance because of their prominence as one of the most common structural system types in the existing tall building inventory in Seattle, and due to concerns regarding the potential for fracture-prone welded connections, which came to light following the 1994 Northridge earthquake. This paper evaluates the response of a representative 1970s 50-story steel moment-resisting frame office building in Seattle under 30 simulated scenarios of a magnitude-9 Cascadia Subduction Zone earthquake. The resulting probability of collapse, conditioned on the M9 scenarios considered, is 42%. This collapse risk is greater than the 25% probability of collapse for the 975-year return period probabilistic estimate of the hazard, and it is below the 85% probability of collapse for the risk-targeted Maximum Considered Earthquake (MCE_R), when basin effects are considered. The estimated collapse risk exceeds by a factor of 8.5 the 10% or less probability of collapse under MCE_R ground motions targeted by modern codes for new design. These high collapse risks are largely driven by: (i) deep sedimentary basin effects, which amplify long period shaking; and (ii) the expected brittle behavior of fracture-prone welded beam-to-column connections. The performance of the building under the M9 scenarios outside of the basin or with ductile beam-to-column connections result in a negligible probability of collapse.

Keywords: Steel Moment-Resisting Frames, Tall Buildings, Cascadia Subduction Zone, Basin Effects

INTRODUCTION

Since the 1906 San Francisco earthquake, structural engineers generally regarded steel moment-resisting frame systems as being among the most ductile and reliable seismic force-resisting systems for buildings [1]. The common view was that when subjected to earthquake shaking, moment-resisting frames would experience only localized damage due to ductile yielding of members and connections. This led to widespread construction of this system, particularly in the high seismic regions of the western United States [1]. The 1994 Northridge earthquake dramatically changed perceptions of the performance of such frames, when post-earthquake inspections revealed cracking in the beam-to-column joint welds in several dozens of low- and mid-rise steel-frame buildings.

Since the late 1950s, Seattle's skyline has changed dramatically with the construction of tall buildings in the downtown area. Among the multi-faceted earthquake risks facing the city, the concentration of tall buildings and infrastructure in the densely populated downtown neighborhood raises questions about the risks to life, property, and recovery from large earthquakes. As a first step towards addressing these questions, this study developed an inventory of tall buildings (10 stories or more) in Seattle. The inventory classifies tall buildings in terms of height, age, use, and structural system characteristics. Although not the only earthquake risk, tall buildings are of special concern due to their size and large occupant loads, where earthquake damage to one tall building can have disproportionate effects on its occupants, its neighbors, and the community at large.

The Seattle tall building inventory identifies more than 50 tall (10 stories and above) steel buildings constructed between 1960 and 1994, the majority of which are moment-resisting frames. These buildings are of interest due to: (1) their prominence as one of the most common structural system types in the tall building inventory; (2) their design, which followed an equivalent lateral force procedure based on the first-mode translation response, without capacity design principles that protect against story mechanisms, and lower base-shear strengths than those specified in modern building codes; and (3) concerns regarding the potential for fracture-prone welded connections, which came to light following the 1994 Northridge earthquake.

Tall buildings are most susceptible to long-period and long-duration ground motions, which are characteristic of large magnitude subduction earthquakes. The vulnerability of these structures is compounded by sedimentary basins, which tend to increase the intensity of earthquake ground motions at long periods and the resulting damage in tall structures. This issue is particularly important in Seattle, which lies above a deep sedimentary basin, and has the potential for large magnitude earthquakes that can dominate the seismic hazard at long periods due to the nearby Cascadia Subduction Zone.

This study aims to evaluate the impact of deep basins during large magnitude subduction earthquakes on the response of pre-1994 tall steel moment-resisting frame buildings in Seattle. Based on data from the tall building inventory, a 1970s 50-story steel moment-frame archetype building is used in this study. The archetype building is subjected to 30 simulated scenarios of a magnitude-9 (M9) Cascadia Subduction Zone interface earthquake, recently generated by Frankel et al. [2] for an average (top 30 m) soil velocity of 600 m/s. Marafi et al. [3] modified these motions to make them consistent with an average velocity of 500 m/s, which is typical of downtown Seattle.

To benchmark building performance under the M9 scenarios against probabilistic estimates of the hazard, which include crustal, intraslab, and interface earthquake sources, building response is also evaluated at intensities of ground motion shaking corresponding to return periods of 975 years and the risk-targeted Maximum Considered Earthquake (MCE_R) defined in building codes (~2000 year return period in Seattle). These hazard estimates explicitly account for basin effects as currently implemented in the design of modern tall buildings in Seattle.

To isolate deep basin effects, the response during the M9 simulations is also evaluated for the town of La Grande (73 km south of Seattle). This location is outside of the deep sedimentary basin, but has a similar distance to the fault-rupture plane as the Seattle site [3]. Building response is also evaluated under the 975-year and MCE_R hazard estimates without consideration of basin effects.

The impact of fracture-prone welded connections on the predicted building response is also quantified by re-evaluating the M9 Cascadia Subduction Zone simulations for Seattle (i) without fracture-prone beam-to-column connections, (ii) without fracture-prone column splices, and (iii) with ductile beam-to-column and splice connections throughout the building.

BUILDING DESCRIPTION AND ANALYSIS MODEL

The archetype building is designed in accordance with the provisions of UBC 1973 [4] and the SEAOC Bluebook of 1973 [5] which was commonly employed to supplement minimum design requirements. The building occupancy is that of a commercial office, with two levels for mechanical equipment, one at mid-height, and one at the top floor. The frames are made up of built-up box columns (denoted R in Figure 1a), wide flange beams, and welded beam-to-column connections. Typical story heights and beam spans are 3.8 m and 8.5 m, respectively. In the 1970s, it was customary to have moment connections in all beam-to-column intersections, as illustrated in Figure 1b. The resulting section sizes for a typical frame are shown in Figure 1a. The archetype building has a total building dead load of 784,220 kN. The design wind and seismic base shears are equal to 1.80% and 1.96% of total building dead load, respectively. The wind and seismic drift limits used in design are 0.0025 and 0.005 respectively. For a detailed description of the design method and assumptions please refer to [6].

In order to conduct nonlinear dynamic analysis of the archetype building, finite element models capable of capturing the response of all structural elements that significantly contribute to the strength and stiffness of the system were developed, consistent with those developed by Molina Hutt et al. [7, 8]. A two-dimensional numerical model of a representative frame, developed in LS-DYNA [9], is illustrated in Figure 1a. The first (T₁), second (T₂) and third (T₃) modes of the representative two-dimensional frame are 5.48, 2.12 and 1.26 seconds, respectively.

Key structural elements include beams, columns and panel zones. Beams are modelled as lumped-plasticity beam elements following recommendations in [10], which propose empirical relationships for modelling steel beams, based on a large database of experiments. To account for fracture in the moment connections, a plastic rotation threshold at which fracture is set to occur in the connections is introduced according to ASCE 41 recommendations [11]. The impact of introducing the plastic rotation threshold at fracture is observed by comparing the hysteretic response for a post- versus pre-Northridge sample moment connection, illustrated in Figure 1c versus 1d.

Columns are modelled as lumped plasticity beam elements with yield surfaces capable of capturing interactions between bending moment and axial force following the recommendations in [12], calibrated based on experimental tests of tubular steel columns in [13], which account for different rates of degradation in the moment-rotation response of columns as a function of axial load-to-capacity ratios. Column splices are modeled by inserting lumped plasticity hinges with strengths equal to the expected splice strength under tension and/or bending. Splices are capable of reaching their expected capacity followed by brittle failure. Full column capacity is assumed in compression since this is achieved by direct bearing. Panel zones are modeled using the Krawinkler model as outlined in [14], which incorporates an assembly of rigid links and rotational springs to represent the true dimensions of the panel zone. For a detailed description of the nonlinear dynamic analysis model please refer to [6].

SEISMIC HAZARD AND GROUND MOTION SELECTION

Frankel et al. [2] produced 30 sets of broadband (0-10 Hz) synthetic seismograms for M9 Cascadia subduction zone earthquakes by combining synthetic seismograms derived from 3D finite-difference simulations (≤ 1 Hz) with finite-source, stochastic synthetics (≥ 1 Hz). These three-dimensional simulations, which consider a variety of rupture parameters to determine the range of expected ground motions, are used in this study. The resulting ground motion spectra for sites not in sedimentary basins (e.g. La Grande), were consistent with existing ground motion models (GMM) [15]. However, response spectra from the synthetics at sites within sedimentary basins (e.g. Seattle) show amplification factors of 2-5 at periods of 1-10 s. These large amplifications are apparent in Figure 2 by comparing the differences in the average response spectrum of the Seattle versus La Grande M9 ground motion suites. Because each simulation has two ground motion components (North-South and East-West), each component is input independently to the two dimensional model.

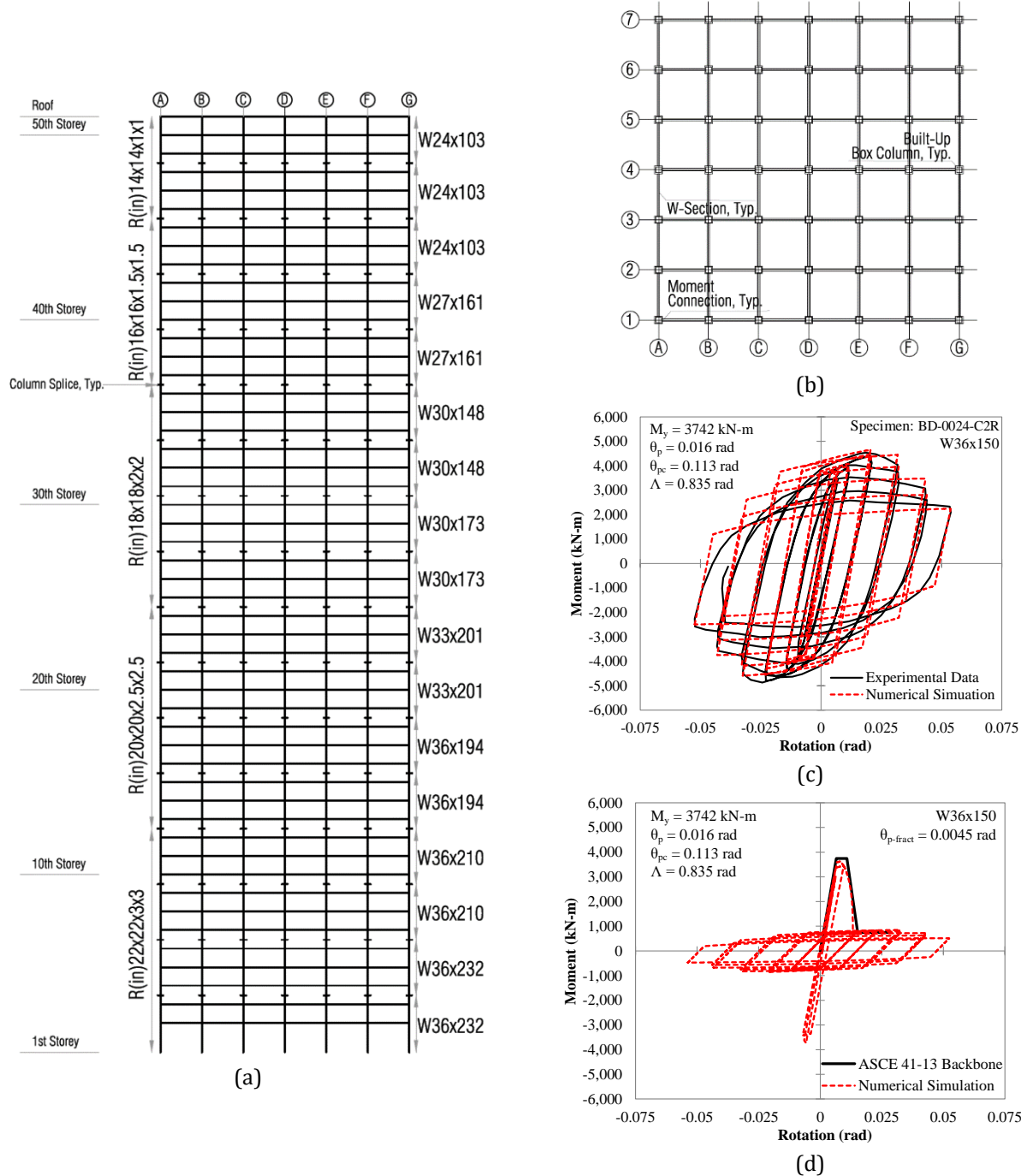


Figure 1: Archetype steel moment-frame building (a) elevation, (b) plan, and sample hysteretic responses of (c) ductile vs (d) fracture-prone beam-to-column connections. Adapted from [8].

To benchmark response during the M9 scenarios against probabilistic estimates of the hazard, the building is also evaluated at intensities of ground motion shaking with return periods of 975 years and the MCE_R defined in building codes. Conditional Spectra (CS) are developed at these two intensities of ground motion shaking, conditioned at the fundamental period of the building.

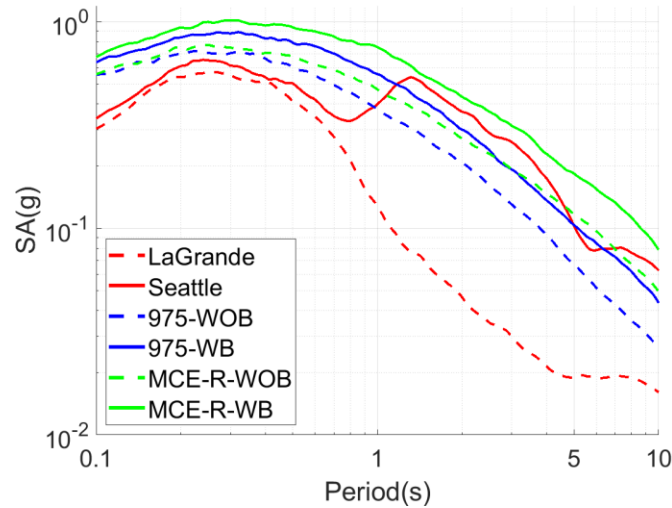


Figure 2: Average response spectra of ground motion suites considered in the assessment, including simulated M9 (Seattle and LaGrande), and ground motion shaking (with -WB- and without -WOB- basin effects) consistent with a 975-year return period and MCE_R shaking.

Ground motions are selected to match the target mean and variance conditional spectra in the maximum direction. Crustal, intraslab, and interface ground motions are included in each suite in proportion to their contribution to their overall seismic hazard at the conditioning period. Out of 99 ground motions in the 975-year suite, 37 are crustal, 57 interface and 5 intraslab. Out of 100 ground motions in the MCE_R suite, 35 are crustal, 62 interface and 3 intraslab. These values were computed using the hazard deaggregation from the codes used to generate the 2014 National Seismic Hazard Maps in the US [16].

For consistency with current practice in Seattle for buildings above 73 m (~240 ft), the spectra are scaled to account for basin amplification, as outlined in [3]. The basin amplification is calculated with the Campbell and Bozorgnia [17] basin term assuming a depth to soils with shear-wave velocities of 2.5 km/s (Z2.5) of 7 km for the Seattle site. The resulting amplification factor at the fundamental period of the building is approximately 1.6, considerably lower than that observed from the M9 simulations, which have an average amplification factor of 4.3 at the fundamental period of the archetype building.

The response of the archetype building is evaluated under a total of 520 ground motion records grouped into six ground motion suites: (1) La Grande M9 simulations (“La Grande”); (2) Seattle M9 simulations (“Seattle”); (3) 975-year return period conditional spectra without basin effects (“975-WOB”); (4) 975-year return period conditional spectra with basin effects (“975-WB”); (5) MCE_R conditional spectra without basin effects (“ MCE_R -WOB”), (6) MCE_R conditional spectra with basin effects (“ MCE_R -WB”). Figure 3 provides a comparison of key ground motion parameters for each suite, including arias intensity (I_a), significant duration ($D_{s5-95\%}$), spectral acceleration at the fundamental period ($S_a(T_1)$) and spectral acceleration at the second mode of vibration ($S_a(T_2)$) of the archetype building. Figure 3 highlights considerable differences in the ground motion properties of the La Grande and Seattle M9 simulation suites. Furthermore, it highlights the impact of considering basin effects in probabilistic seismic hazard calculations, e.g. the ground motion properties of the 975-WB suite are consistent with those of the MCE_R -WOB suite. The selected ground motions are input at the base of the analytical model, which is assumed to be fixed at its base. A damping ratio of 2.5% is assumed in the analysis [18].

RESULTS AND DISCUSSION

The results suggest there are considerable variations in performance depending on whether the archetype building is located inside vs outside of the basin. The simulated M9 scenarios with basin effects (Seattle) result in a 42% chance of collapse. Response under probabilistic estimates of the hazard, with consideration of basin effects, indicate there is a 25% chance of collapse under shaking intensities with a 975-year return period, and 85% collapse probability under MCE_R shaking. In contrast, the simulated M9 scenarios without basin effects (La Grande) result in negligible collapse risk. Response under probabilistic estimates of the hazard, without consideration of basin effects, indicate there is a 4% chance of collapse under shaking intensities with a 975-year return period, and 32% collapse probability under MCE_R shaking.

Collapse probabilities and median response parameters including story drifts, peak floor accelerations, beam plastic rotation, column plastic rotation, splice plastic rotations, panel zone total rotations and normalized base shear for all ground motion suites considered in the study are summarized in Table 1. The results suggest the M9 ground motion simulations with basin effects fall within the 975-year and MCE_R estimates of the hazard. Comparison of M9 simulation results inside and outside the basin highlight a drastic impact of basin amplification on seismic risk to existing tall steel moment frame buildings. Contrasting probabilistic estimates of the hazard with and without consideration of basin effects also highlight how neglecting basin effects can significantly underestimate collapse risk by a factor of 6.3 at shaking with a 975-year return period, and a factor of 2.65 at MCE_R . The trends observed are consistent with a similar study that evaluated the response of representative reinforced concrete shear-wall systems [3]. Figure 4 illustrates median results of beam plastic rotation and story drift up the building height for all ground motion suites considered in the assessment. The results highlight a significant concentration of deformation in a small number of stories (particularly at the upper stories). The results under MCE_R shaking with basin effects are not seen in the figure, because median runs result in collapse. Beam plastic rotation results follow closely the story drift trends, indicating that deformations can be primarily attributed to nonlinear response in the beams.

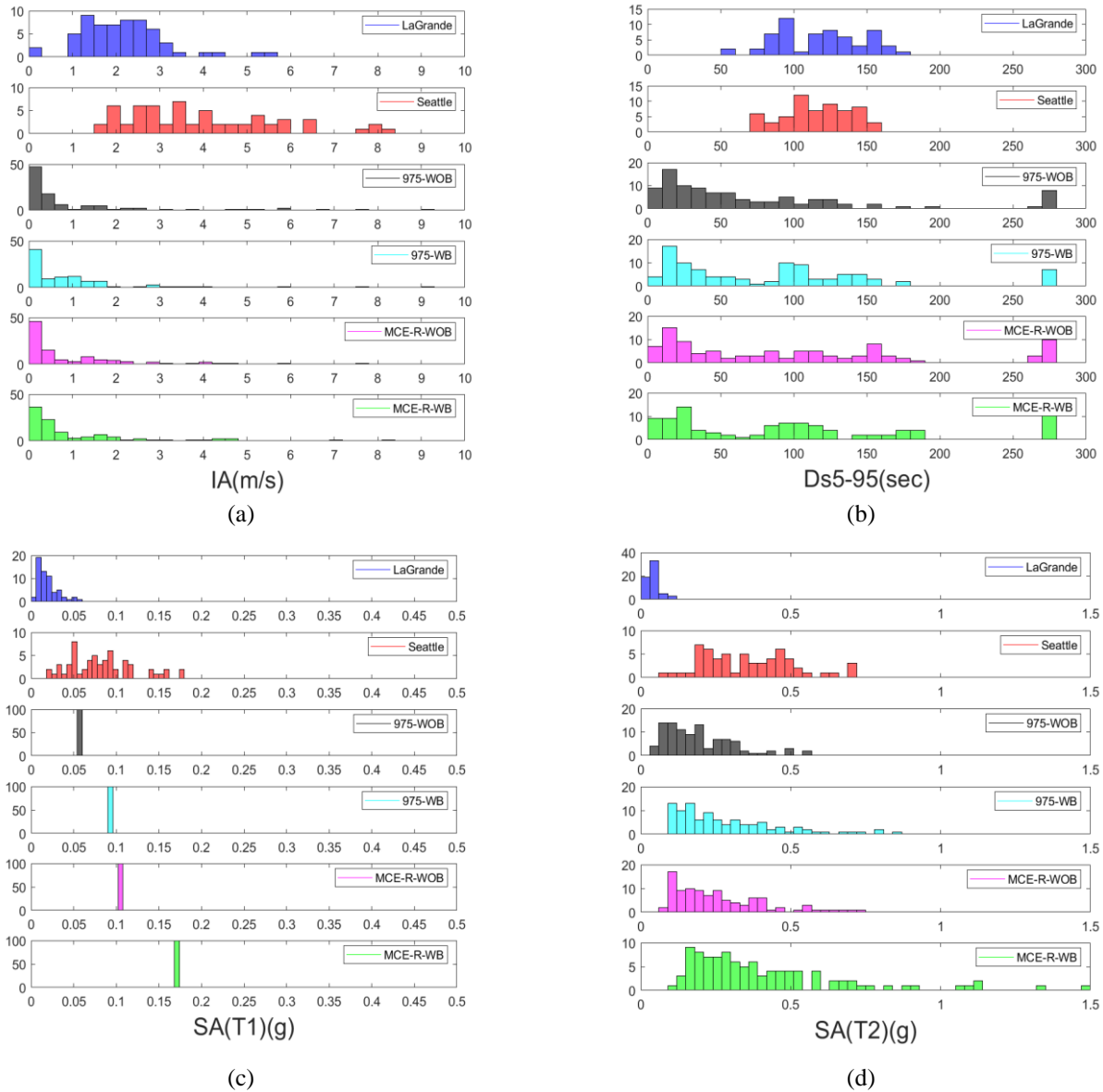


Figure 3. Histogram plots of (a) arias intensity (I_a), (b) significant duration ($D_{s5-95\%}$), (c) spectral acceleration at fundamental period ($S_a(T_1)$), and (d) spectral acceleration at second period ($S_a(T_2)$), for ground motion suites considered in the assessment, including simulated M9 (Seattle and LaGrande), and ground motion shaking (with -WB- and without -WOB- basin effects) consistent with a 975-year return period and MCE_R shaking.

Table 1: Median results of ground motion suites considered in the assessment, including simulated M9 (Seattle and La Grande), and ground motion shaking (with and without basin effects) consistent with a 975-year return period and MCE-R shaking. “Collapse” indicates that 50% or more of the ground motions in the suite caused the structure to collapse.

| Suite | $P_{collapse}$ [Total # of runs] | Story Drift (%) | Peak Floor Acceleration (g) | Beam Plastic Rotation (rad) | Column Plastic Rotation (rad) | Splice Plastic Rotation (rad) | Panel Zone Total Rotation (rad) | Normalized Based Shear (-) |
|--------------|-------------------------------------|-----------------|-----------------------------|-----------------------------|-------------------------------|-------------------------------|---------------------------------|----------------------------|
| La Grande M9 | 0% [60] | 0.38 | 0.26 | 0.000 | 0.0000 | 0.0003 | 0.0004 | 0.022 |
| Seattle M9 | 41.7% [60] | 3.48 | 0.69 | 0.026 | 0.0003 | 0.0021 | 0.0014 | 0.100 |
| 975-WOB | 4.0% [99] | 1.20 | 0.43 | 0.000 | 0.0000 | 0.0007 | 0.0009 | 0.062 |
| 975-WB | 25.3% [99] | 1.81 | 0.61 | 0.005 | 0.0003 | 0.0012 | 0.0013 | 0.100 |
| MCE-R-WOB | 32% [100] | 2.17 | 0.67 | 0.010 | 0.0010 | 0.0015 | 0.0014 | 0.098 |
| MCE-R-WB | 85% [100] | Collapse | Collapse | Collapse | Collapse | Collapse | Collapse | Collapse |

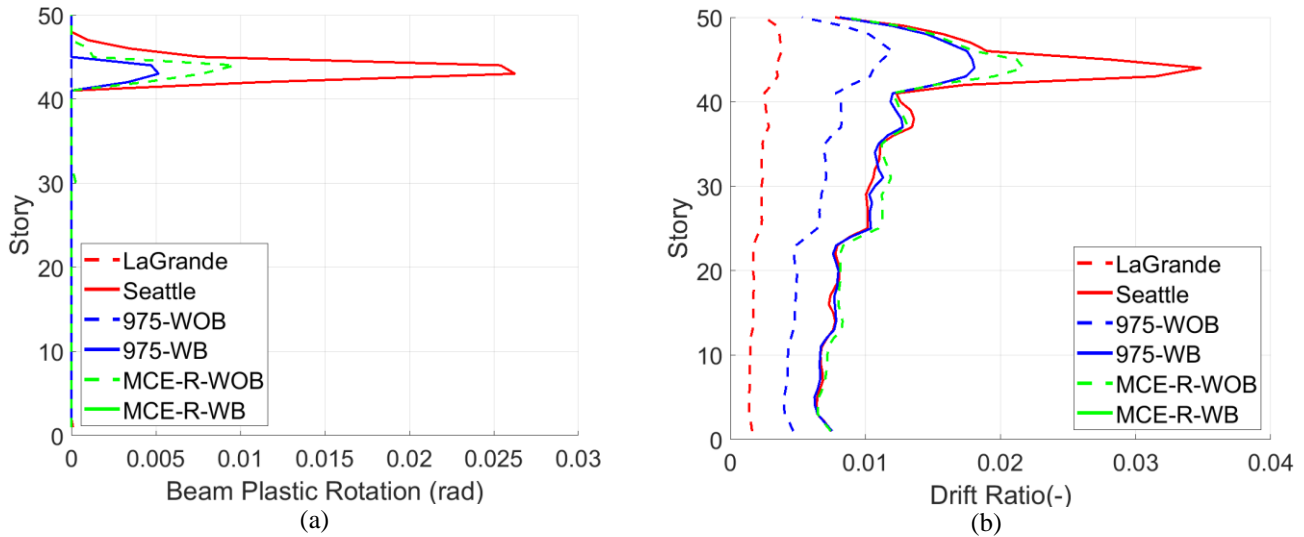


Figure 4: Median (a) plastic rotation of the beams and (b) story drift ratio results of ground motion suites considered in the assessment, including simulated M9 (Seattle and LaGrande), and ground motion shaking (with -WB- and without -WOB- basin effects) consistent with a 975-year return period and MCE-R shaking.

To investigate the impact of fracture-prone welded connections on overall building response, three additional structural models are developed to benchmark against the baseline case (“Brittle” model in Table 2). Performance under the M9 ground motions in Seattle is re-assessed assuming (i) fracture-prone beam-to-column connections, but ductile column splices (“beam fracture” model in Table 2), (ii) fracture-prone column splice connections, but ductile beam-to-column connections (“splice fracture” model in Table 2), and (iii) ductile beam-to-column and splice connections throughout the building (“ductile” model in Table 2). Collapse probabilities and other response parameters, as previously presented in Table 1, under the M9 ground motions in Seattle are summarized in Table 2 for the brittle, beam fracture, splice fracture and ductile models. Figure 5 illustrates median results of beam plastic rotation and story drift up the building height for these same models.

The results indicate that the presence of fracture-prone welded connections drives the collapse risk. As previously noted, the probability of collapse when brittle connections are present in both beam-to-column and splice connections under M9 simulations in Seattle is 42%. Retrofitting splice connections to have a ductile response would decrease the collapse risk to

33%, whereas retrofitting beam-to-column connections to have a ductile response would eliminate the collapse risk under the M9 scenarios considered. The analysis results assuming retrofitted splice and beam-to-column connections to have ductile response coincide with those of only retrofitting beam-to-column connections, which suggests that the effect of brittle splices is significant only when coupled with fracture-prone connections.

Table 2: Median of Seattle M9 simulation results for structural models with and without beam-to-column and column splice fracture-prone welded connections.

| Model | Suite | $P_{collapse}$ [Total # of runs] | Story Drift (%) | PFA (g) | Beam Plastic Rotation (rad) | Column Plastic Rotation (rad) | Splice Plastic Rotation (rad) | Panel Zone Total Rotation (rad) | Normalized Based Shear (-) |
|--------------------|---------------|--|-----------------------|------------|--------------------------------------|--|--|--|-------------------------------------|
| Brittle | Seattle M9 | 42% [60] | 3.48 | 0.69 | 0.026 | 0.0003 | 0.0021 | 0.0014 | 0.100 |
| Beam Fracture | Seattle M9 | 33% [60] | 2.72 | 0.64 | 0.016 | 0.0000 | 0.0019 | 0.0014 | 0.099 |
| Splice Fracture | Seattle M9 | 0% [60] | 2.31 | 0.54 | 0.011 | 0.0000 | 0.0017 | 0.0015 | 0.101 |
| Ductile | Seattle M9 | 0% [60] | 2.31 | 0.54 | 0.011 | 0.0000 | 0.0017 | 0.0015 | 0.101 |

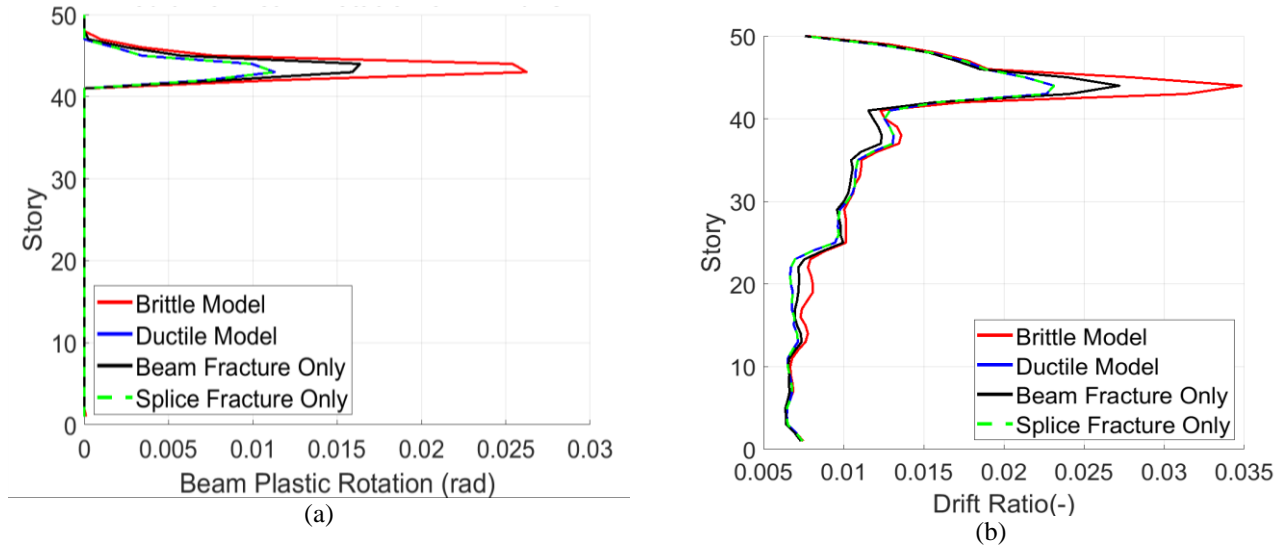


Figure 5: Median (a) plastic rotation of the beams and (b) story drift ratio results of Seattle M9 simulations for structural models with and without beam-to-column and column splice fracture-prone welded connections.

CONCLUSION

This paper evaluates the response of a 1970s 50-story steel moment-resisting frame office building (with welded beam-to-column connections) in Seattle under 30 simulated scenarios of a M9 Cascadia Subduction Zone earthquake. Collapse risk of the archetype building under the M9 scenarios considered is unacceptably high at 42%. The simulation results fall within the 975-year return period probabilistic estimate of the hazard and MCE_R shaking, which have a 25% and 85% probability of collapse, respectively, when basin effects are considered. These estimates exceed by a factor of 8.5 the code target of 10% or less probability of collapse under MCE_R shaking. These high collapse risks are largely driven by (i) the effects of the deep sedimentary basin, which amplify long period shaking, and (ii) fracture-prone welded beam-to-column connections.

ACKNOWLEDGEMENT

The authors would like to thank The University of British Columbia’s Cascadia Engagement Fund for supporting this collaboration with The University of Washington.

REFERENCES

- [1] FEMA (2000). "State of the Art Report on Past Performance of Steel Moment-Frame Buildings in Earthquakes." FEMA 355-E, Federal Emergency Management Agency, Washington, DC.
- [2] Frankel, A. D., Wirth, E. A., Marafi, N. A., Vidale, J. E., Stephenson, W. J. (2018). "Broadband Synthetic Seismograms for Magnitude 9 Earthquakes on the Cascadia Megathrust Based On 3D Simulations and Stochastic Synthetics (Part 1): Methodology and Overall Results." *The Bulletin of the Seismological Society of America*, 108 (5A): 2347–2369.
- [3] Marafi, N. A., Makdisi, A. J., Eberhard, M. O., Berman, J. W. (2018). "Impacts of M9 Cascadia Subduction Zone Earthquake and Seattle Basin on Performance of RC Core-Wall Buildings." *Journal of Structural Engineering*, under review.
- [4] UBC (1973). "Uniform building code 1973 edition." UBC 73, International Conference of Building Officials, Whittier, CA.
- [5] SEAOC (1973). "Recommended lateral force requirements and commentary." Seismology Committee, Structural Engineers Association of California, Sacramento, CA.
- [6] Molina Hutt C. (2017). "Risk-based seismic performance assessment of existing tall steel framed buildings." Ph.D. Dissertation, University College London (UCL), London, UK.
- [7] Molina Hutt, C., Almufti, I., Willford, M., and Deierlein, G. (2016). "Seismic Loss and Downtime Assessment of Existing Tall Steel-Framed Buildings and Strategies for Increased Resilience", *ASCE Journal of Structural Engineering*, vol. 142, no. 8, pp. C4015005:1-17.
- [8] Molina Hutt, C., Rossetto T. and Deierlein, G. (2018). "Comparative risk-based seismic performance assessment of 1970s vs modern tall steel moment resisting frames." *Earthquake Engineering and Structural Dynamics*, under review.
- [9] LSTC (2011). [Computer software]. LS-DYNA, Livermore Software Technology Corporation, Livermore, CA.
- [10] Lignos, D. and Krawinkler, H. (2011). "Deterioration Modeling of Steel Components in Support of Collapse Prediction of Steel Moment Frames under Earthquake Loading". *Journal of Structural Engineering*, 131(11): 1291-1302.
- [11] ASCE (2013). "ASCE-41: Seismic Evaluation and Retrofit of Existing Buildings." ASCE/Structural Engineering Institute (SEI) 41-13, Reston, VA.
- [12] Lignos, D. and Krawinkler, H. (2010). "A steel database for component deterioration of tubular hollow square steel columns under varying axial load for collapse assessment of steel structures under earthquakes." Joint Conference Proc., 7th International Conference on Urban Earthquake Engineering & 5th International Conference on Earthquake Engineering, Tokyo Institute of Technology, Tokyo, Japan.
- [13] Kurata, M., Suita, K. and Nakashima, M. (2005). "Test on large cyclic deformation of steel tube columns having fixed column bases." *Journal of Structural and Construction Engineering*, 598:149-154.
- [14] PEER (2010). "Modeling and acceptance criteria for seismic design and analysis of tall buildings." PEER Report 2010/111 also published as PEER/ATC-72-1, Pacific Earthquake Engineering Research Center, University of California, Berkeley, CA.
- [15] Abrahamson, N., Gregor, N., and Addo, K. (2016). "BC Hydro Ground Motion Prediction Equations for Subduction Earthquakes." *Earthquake Spectra* 32(1): 23–44.
- [16] USGS (2018). "National Seismic Hazard Mapping Project (NSHMP) Code". <<https://github.com/usgs/nshmp-haz>>
- [17] Campbell, K. W. and Bozorgnia, Y. (2014). "NGA-West2 Ground Motion Model for the Average Horizontal Components of PGA, PGV, and 5% Damped Linear Acceleration Response Spectra." *Earthquake Spectra* 30(3): 1087–1115.
- [18] PEER-TBI (2017). "Tall Buildings Initiative: Guidelines for Performance-based Seismic Design of Tall Buildings." PEER Report 2017/06, Pacific Earthquake Engineering Research Center, University of California, Berkeley, CA.